Int J Thermophys (2008) 29:2200–2205
DOI 10.1007/s10765-007-0262-3

Photopyroelectric Microscopy of Plant Leaves

B. R. Briseño-Tepepa · J. L. Jiménez-Peréz · R. Saavedra · R. González-Ballesteros · E. Suaste · A. Cruz-Orea

Published online: 25 September 2007

Abstract The use of photothermal microscopy to obtain superficial and in-depth images, by means of the interaction of a thermal wave with the analyzed material, has reached great interest due to its numerous applications. The application of the photopyroelectric microscopy technique to obtain images of plant leaves is presented in this article. In the experimental setup, a pyroelectric sensor and linear micro-positioners were used to obtain the photothermal signal at each point of the sample. Then it is possible to obtain images of plant leaves through their differences in local thermal properties and thickness.

Keywords Ligustrum japonicum leaf · Photoacoustic microscopy · Photopyroelectric microscopy · Photothermal techniques · Thermal-wave imaging · Thin-film photopyroelectric detection

B. R. Briseño-Tepepa · J. L. Jiménez-Peréz
Centro de Investigacion en Ciencia Aplicada y Tecnología Avanzada, IPN Calz. Legaria 694, Col. irrigación, 11500 México, D.F., México

R. Saavedra
Departamento de Física, Universidad de Concepción, Casilla 160C, Concepcion, Chile

R. González-Ballesteros
Universidad Politécnica de Pachuca, Km 20 de Carr. Pachuca-Cd. Sahagún, Zempoala, Hgo, México

E. Suaste
Sección de Bioelectrónica, Departamento de Ingeniería Eléctrica, CINVESTAV-IPN, Av. IPN No. 2508, Col. San Pedro Zacatenco, C.P. 07360 México, D.F., México

A. Cruz-Orea (✉)
Departamento de Física, Centro de Investigación y Estudios Avanzados del IPN, Av. IPN No. 2508, Col. San Pedro Zacatenco, C.P. 07360 México, D.F., México
e-mail: orea@fis.cinvestav.mx

1 Introduction

Thermal waves are used nowadays for non-destructive evaluation of various types of surface and sub-surface features. In thermal-wave imaging, macroscopic and microscopic thermal features on or beneath the surface of a sample can be detected and imaged. Thermal features can be defined as those regions of an otherwise homogeneous material that exhibit variations, relative to their surroundings, in any of the following three thermal parameters: density, ρ; specific heat, c; and thermal conductivity, k. Variations in these thermal parameters arise, in the most general sense, from variations in the local structure of the material. Imaging of these local thermal features requires detection of the scattered and reflected thermal waves [1].

This detection is currently accomplished by several photothermal (PT) techniques. These techniques involve measurements of the heat produced, as an excited species relaxes by a nonradiative path. The excited light is chopped at a suitable frequency, and the resulting modulated heat flow is detected by using a direct or indirect temperature sensor, and a lock-in amplifier. These techniques allow the acquisition of information about samples with inherent difficulties such as high dispersion of light and structures that vary with depth (for example, semiconductors, minerals, vegetables, and animal tissue).

PT techniques have been used since 1979 to obtain thermal images from different samples, being a nondestructive technique. Among the PT techniques, the photoacoustic technique was the first to be used to obtain thermal images. Photoacoustic microscopy (PAM) is a well established and useful tool in the nondestructive testing of materials. There has been considerable interest in employing PAM for surface and sub-surface imaging, and microscopy of solid materials. The unique characteristic of photoacoustic imaging lies in the detection of subsurface features or flaws by the interaction of the photoacoustically generated thermal waves with these features [2]. This characteristic to detect surface, and subsurface defects makes PAM particularly valuable in locating voids and cracks in metals, ceramics, and semiconductors.

Briefly, the technique involves modulating the intensity of a focused laser beam, and slowly scanning the position of the beam across the sample of interest. The thermal waves generated in the sample by the periodic heating scatter off defects below the surface of the sample, and this causes a change in the photoacoustic signal. As the laser beam is scanned across the sample, any change in the photoacoustic signal indicates the presence of defects at that location [3].

Different researchers have used PT techniques to detect inhomogeneous structures such as diffused and ion-implanted regions in semiconductors [4], and integrated circuits [5]. Unlike these, there are few reports on imaging applications using a pyroelectric (PE) sensor. The emergence of thin-film photopyroelectric (PPE) detection as a convenient photothermal method, with considerably more degrees of freedom than photoacoustic imaging (both microphonic and piezoelectric), and a back—detection character, as opposed to the photothermal—beam deflection front —detection character, has been well documented. Conventional pyroelectric detection of thermal waves used in a scanned, spatially integrated detection mode has also been reported.

Imaging of the thermal wave field with a polyvinylidene-difluoride (PVDF) pyroelectric sensor in the back detection configuration (in this case, the modulated light

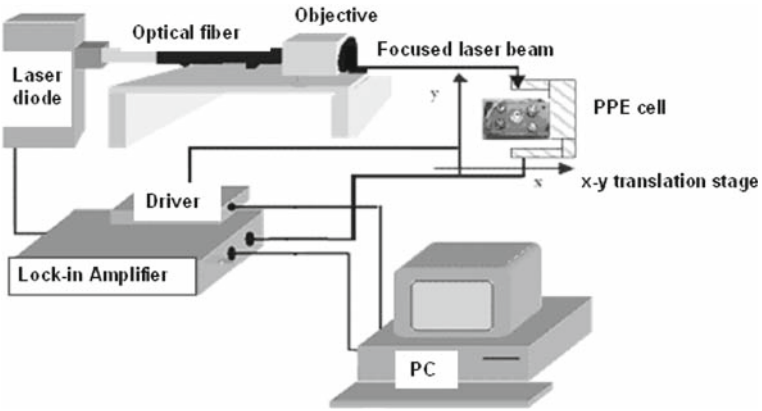

Fig. 1 Experimental setup used to obtain PT images of biological samples

impinges the sample, and the PE sensor is attached to the other side of the sample) was demonstrated [6]. Recently, imaging with a PE sensor was reported, but in this case, in a front detection configuration (the modulated light impinges the PE sensor, and the sample is attached on the other side of the sensor [7]). In the present study, we are interested in the use of a PE sensor to obtain images from plant leaves by using back and front PPE configurations.

2 Experimental Setup

A schematic diagram of the detection experimental setup used for PPE scanned imaging is shown in Fig. 1. In this arrangement, the excitation source is a fiber coupled laser diode, with variable power at 650 nm wavelength, modulated in intensity at a frequency (f) of 2 Hz, by the reference oscillator of a DSP lock-in amplifier. By using a microscope objective, the laser beam was focused on the leaf sample (the spot size of the laser was approximately 50 μm). The sample was a *Ligustrum japonicum* leaf, which has 6–8 pairs of veins in the blade and a central main vein (midrib); these veins and midrib are somewhat sunken on the back side of leaf, whereas the front side of this leaf is a quite flat surface.

A piece of this leaf, cut from its root, was immediately placed inside the PPE cell. The PE sensor, a 25 μm thickness PVDF, was uniformly covered with a thin and homogeneous layer of silicon oil (approximately 20 μm thickness) to ensure good thermal contact between the sensor and sample. The PPE cell is mounted on an x–y translation stage, with a resolution of 50 μm, driven by stepping motors. The PPE signal was preamplified, and sent to the DSP lock-in amplifier. A personal computer was used to control scanning of the x–y translation stage, and also to record from the lock-in amplifier, the experimental PPE signal amplitude and phase from each point of the scanned sample. PT images of the leaf samples with the PPE cell in the back and front detection configurations were obtained.

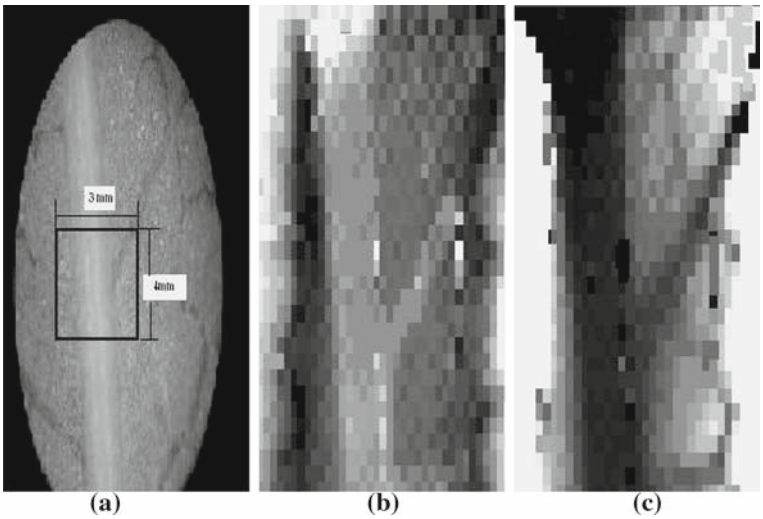

Fig. 2 (**a**) Microscopic image of sample. Delimited area shows scanned area for (**b**) PPE signal amplitude, and (**c**) PPE signal phase obtained from the PPE back detection configuration

3 Results and Discussion

Figure 2 shows (a) a microscopic picture of the *Ligustrum japonicum* leaf and its PT image from (b) the PPE signal amplitude and (c) phase. In this case, the back detection configuration was used with 15.5 mW laser power. After acquisition of the PPE signal, it was observed that any thermal damage, as a consequence of the focused laser beam scanning, occurred on the leaf. From the PPE amplitude and phase, it is possible to observe images of the leaf midrib (main vein) and blade. Both images show an internal channel in the midrib, which is not possible to observe from (a) the microscopic picture.

An image of a *Ligustrum japonicum* leaf was also obtained for the front detection configuration in order to have the possibility of increasing the laser power (to 24 mW) without causing thermal damage to the plant leaf, due to the fact that now the focused laser beam impinges on the sensor surface. In this configuration, the thermal information is not altered by the optical properties of the sample [7]. Figure 3 shows a microscopic picture of (a) the leaf and (b) its image from the PPE signal phase. From the PPE image, it is also possible to observe the main parts of the leaf, the midrib, blade, and an internal channel in the midrib as for the case of the former configuration.

The thermal properties of leaf are not homogeneous, which means that the sample have thermal variations in its structure, due to the fact that is formed by several layers and channels; also, the sample has thickness variations in its main parts, which makes it possible to use the PPE technique to observe the main leaf features, since the PPE signal depends on the sample's thermal characteristics and thickness. Next, the thermal and optical conditions of the leaves with the PPE measurements are described.

The reported thermal diffusivity (α) for vegetal leaves is about $1.2 \times 10^{-3}\,\mathrm{cm}^2 \cdot \mathrm{s}^{-1}$ [8], and an individual *Ligustrum japonicum* leaf has thicknesses varying from 195 to

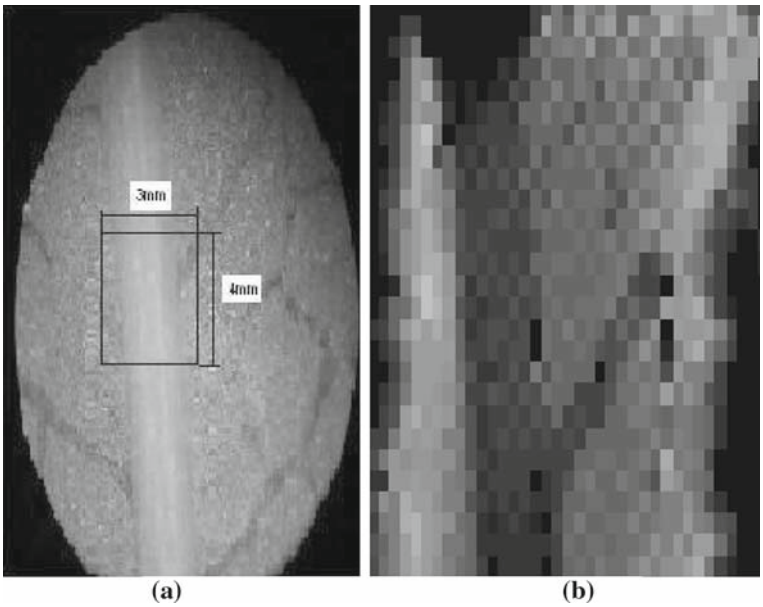

Fig. 3 (**a**) Microscopic image of the sample. Delimited area shows scanned area for (**b**) PPE signal phase obtained from the PPE front detection configuration

635 μm, from the blade to the midrib parts, respectively. Then, for a light modulation frequency (f), of 2 Hz, the sample is thermally thick, which means that $L_s/\mu_s > 1$, where L_s is the sample thickness and μ_s is the thermal diffusion length defined as $\mu_s = (\alpha/\pi f)^{1/2}$. Also, the sample is optically opaque at the laser wavelength (650 nm) used here, since the leaves contain chlorophyll, and one of the optical absorption peaks, corresponding to chlorophyll B, is located at 650 nm [9]. For this peak, the optical absorption coefficient (β) is 190 cm^{-1} [8]; then, $\beta L_s > 1$, which means that the sample is optically opaque. On the other hand, the pyroelectric sensor is optically opaque and thermally thin by taking into account the optical and thermal parameters for a PVDF pyroelectric sensor [7]. In both detection configurations, the front side of the leaf, which is quite flat, is thermally coupled to the pyroelectric sensor by a thin layer of silicon oil (around 20–40 μm thickness), then, by taking into account the light modulation frequency (f) and the reported thermal diffusivity for this silicon oil [7], this coupling layer is thermally thin, which means that this oil layer is thermally transparent for the obtained images.

Under these conditions of optically opaque sample and sensor, with the sensor and coupling oil layer thermally thin, and the sample thermally thick, the PPE signal phase shift ($\Delta\varphi$) depends on the sample thickness variation and also on the thermal diffusivity, and can be expressed as [7,10]

$$\Delta\varphi = -a_s \Delta L_s, \tag{1}$$

where $a_s = \mu_s^{-1}$ is the thermal diffusion coefficient. Then Eq. 1 indicates that it is possible to obtain a PPE signal phase shift when the sample varies in its local thermal properties or thickness of its structure. On the other hand, the PPE signal amplitude decreases exponentially when the sample thickness is increased [10]. Then, it is possible to obtain a PT image of samples where thermal and thickness variations take place in their structure, as is the case for many biological tissues. It is important to mention that the resolution of this technique is limited by the spot size of the focused laser beam, used to scan the sample, also the resolution of the x–y stage, and the light modulation frequency (f) along with the sample thermal diffusivity, which determine the thermal diffusion length in the sample. Also, in the back detection configuration, the thickness of the sample is important due to the fact that the PPE signal amplitude decreases exponentially when the sample thickness is increased, and the laser intensity is limited in order to avoid damage in the biological sample.

4 Conclusions

Photothermal images of plant leaves, *Ligustrum japonicum*, were obtained by using a PPE technique. The back and front detection configurations were used to obtain PT images of these leaves. In both configurations, it is possible to obtain the sample image by scanning the modulated laser beam on the sample, and detecting the PPE signal at each point of the scan. The studied leaves have thermal variations in their structure, and also have significant thickness variations in their main parts (midrib and blade), which makes it possible to obtain their images by using the PPE technique. From the PPE amplitude and phase, it was possible to observe images of the leaf midrib and blade. The images obtained from the back and front PPE detection configurations show an internal channel in the midrib, which is not possible to observe in the microscopic picture.

Acknowledgments The authors are thankful to the Mexican Agencies, CONACYT, COFAA, and CGPI for financial support of this work. One of the authors (A. Cruz Orea) is grateful for financial support from CONACYT Project No. 43252-R. We also want to thank Ing. D. Jacinto Méndez, Ing. E. Ayala, Ing. M. Guerrero, and Ing. A. B. Soto for their technical support at the Physics Department, CINVESTAV-IPN.

References

1. A. Rosencwaig, Science **218**, 223 (1982)
2. G. Busse, A. Rosencwaig, Appl. Phys. Lett. **36**, 815 (1980)
3. R.S. Quimby, Appl. Phys. Lett. **45**, 1037 (1984)
4. A. Rosencwaig, R.M. White, Appl. Phys. Lett. **38**, 165 (1981)
5. L.D. Favro, P.K. Kuo, J.J. Pouch, R.L. Thomas, Appl. Phys. Lett. **36**, 953 (1980)
6. M. Mieszkowsky, A. Mandelis, J. Opt. Soc. Am. **7**, 552 (1990)
7. J. van den Brand, M. Chirtoc, M.R. Wubbenhorst, J.H.W. de Wit, J. Appl. Phys. **93**, 2019 (2003)
8. M.V. Marquezini, N. Cella, A.M. Mansanares, H. Vargas, L.C.M. Miranda, Meas. Sci. Technol. **2**, 393 (1991)
9. C.H. Aguilar, A. Carballo, A. Cruz-Orea, R. Ivanov, E. San Martin Martinez, A. Michtchenko, J. Phys. IV **125**, 853 (2005)
10. A. Mandelis, M.M. Zver, J. Appl. Phys. **57**, 4421 (1985)